https://doi.org/10.33472/AFJBS.6.5.2024.7610-7626

African Journal of Biological Sciences

Green Synthesis Of Magnetite Nanoparticles (Fe_3O_4) Using *Acacia Caesia* (L.) Leaf Extract: Characterization, Biological Activities And Cytotoxicity

Manchiraju Padmaja[1&2], Shyamala Pulipaka[1]*

[1]Department of Physical and Nuclear Chemistry and Chemical Oceanography, School of Chemistry, Andhra University, Visakhapatnam-530003, A P, India.
[2]Department of Chemistry, Government College (A), Rajahmundry-533105, Andhra Pradesh and India.

***Corresponding Author**: *Prof. Shyamala Pulipaka*
*Email: shyamalapulipaka06@gmail.com

Article History
Volume 6, Issue 5, May 2024
Received:
Accepted:
Published:
Doi: 10.33472/AFJBS.6.5.2024.7610-7626

Abstract:
In this study, the aqueous extract of *Acacia caesia* leaves was used as a reducing agent and capping agent to synthesize magnetite nanoparticles (Fe_3O_4) or iron oxide nanoparticles (IONPs). The physicochemical properties of Fe_3O_4 NPs were characterized using UV-Vis, FTIR, XRD, FESEM-EDX and HRTEM methods, showing that the NPs had a spherical shape with an average particle size of 69 nm. The functional groups responsible for the reduction of Fe_3O_4 NPs were found using FTIR correlated with phytochemical screening and XRD revealed a face-centered cubic structure. Effective *in vitro* antifungal, antioxidant, and anti-inflammatory activities of Fe_3O_4 have been discovered. DPPH antioxidant activity and albumin denaturation inhibition exhibited lower IC_{50} values than other activities. The cytotoxic activity on HeLa cell lines is considered very effective with an IC_{50} value of 65.30 µg mL^{-1}.

Keywords: Magnetite nanoparticles, *Acacia caesia*, antifungal, antioxidant, anti-inflammatory, cytotoxicity.

INTRODUCTION:

Nanotechnology is an interdisciplinary science led to the revolutionary development in various scientific fields. Nanoparticles can be defined as the materials with any one of its dimensions less than 100nm [1, 2]. The shape, physiochemical, thermal, magnetic, opto-electrical, catalytic properties and reactivity of nanomaterials depends upon their large surface area to volume ratio and ultrasmall size which are differ from their bulk counterparts [3]. Tuning size and shape of the nanomaterials can be achieved by maintaining different parameters during synthesis of nanomaterials eg. pH, Temperature, reducing and capping agent complexity. Conventional routes for the synthesis of nanomaterials involves usage of toxic chemicals, high temperature, and pressure results in increased toxicity to the environment and living organisms, also become expensive process and time consuming [4-6]. To overcome the challenges associated with conventional synthesis

methods, green synthesis methods become advantage because of eco-friendly, biocompatibility and rapid synthesis. The reduction and capping of metal/metal oxide nanoparticles involved use of renewable green resources such as plant and microbial (bacteria, fungi and algae) metabolites [6, 7].

Iron oxide nanoparticles (IONPs) are vital metal oxide nanoparticles with significant applications in biomedical field such as cell imaging, Magnetic Resonance Imaging (MRI), biosensing, cancer therapy, targeted drug delivery [6]. The super magnetic property of IONPs is a promising feature enable them to use these nanomaterials in diagnosis of various diseases. Magnetite and maghemite (Fe_3O_4 and γ-Fe_2O_3) are two important classes of IONPs, out of which Magnetite nanoparticles (Fe_3O_4) are most commonly used IONPs in biomedical applications and typically preferred core is around 10-50nm. IONPs exhibit super paramagnetic behavior with large magnetic moments when it attains blocking temperature [8, 9].

Several studies had been carried out for synthesis of IONPs using various green resources such as *Artocarpus heterophyllus* peel [1], *Ceratonia siliqua* [2], *Hibiscus rosa sinensis* flowers [7] [10], *Ficus carcica* [3] Saffron extract [4], *Psidium guajava* [5], *Coriandrum sativum* [11], *Carcica papaya* [12], *Moringa oleifera* [13], *Bauhinia tomentosa* [14], Tea waste [15], Natural rubber latex [16], *Garcinia mangostana* fruit [17], Boiled leaves of silky hairs and leaves of Chinese cabbage [18], *Borassus flabellifer* seed coat [19], Urease enzyme [20], *Pencillium* fungi [21] and *Chlorella* K01 [22].

Acacia caesia (L.) is a perennial woody, climbing shrub, endemic to South-east Asia and prominent in west ghats of India with rich phytochemistry. The stem bark possess various therapeutic properties such as insecticidal, wound healing, antimicrobial properties and also used as remedy for gastrointestinal disorders in traditional medicine. The leaves used for the treatment of skin disorders, scabies, asthma and menstrual disorders. The recent literature showed the presence of alkaloids, saponins, flavonoids and glycosides in *Acacia caesia* (L.) [23, 24]. The silver nanoparticles synthesized from *Acacia caesia* (L.) leaf extract exhibited considerable insecticidal activity against mosquito vectors [25]. The ZnO nanoparticles synthesized from *Acacia caesia* (L.) stem bark efficiently shown methylene blue photocatalytic degradation, antimicrobial and anti-inflammatory properties [26]. No study has been reported on the synthesis of IONPs using *Acacia caesia* (L.) plant. Therefore, the present study focuses on green synthesis of Fe_3O_4 nanoparticles using *Acacia caesia* (L.) aqueous leaf extract (ACLAE) for evaluation of antifungal, *in vitro* antioxidant, *in vitro* anti-inflammatory properties and cytotoxicity.

2. Materials and Methods

2.1. Materials:

Luria Bertani Broth (LB Broth), Muller Hinton Agar (MHA) 2% glucose W/methylene blue, 2,2-diphenyl-1-picrylhydraxyl (DPPH), Sodium acetate, 2,4,6-tris (2-pyridyl)-S-triazine (TPTZ), Ferric chloride ($FeCl_3$), Ferrous sulphate ($FeSO_4$), Ammonium hydroxide, Potassium persulphate, Azino-bis(3-ethyl benzothiazoline-6-sulfonic acid (ABTS), Bovine Serum Albumin (BSA), Dimethyl sulfoxide (DMSO), Gallic acid, Ascorbic acid, Triphenyl tetrazolium chloride (TTC) and other materials required for evaluation of biological activities were obtained from Himedia Laboratories.

2.2. Instruments:

UV-Vis Spectrophotometer (Shimadzu UV 2600), Fourier Transform Infrared Spectroscopy (FTIR) (Bruker Alpha II), Powder X-ray diffractometer (XRD) (Bruker), Field Emission Scanning Electron Microscope coupled with Energy dispersive X-ray spectrometry (FESEM-EDX) (JOEL), High Resolution Transmission Electron Microscope (HRTEM) (FEI Tecnai G2, F30), Hot air oven (Thermo Scientific), Autoclave (LabTech) and Laminar Air Flow (BSL-2) (Thermo Scientific).

2.3. Collection and Preparation of *Acacia caesia* leaf aqueous extract (ACLAE):

The fresh leaves of *Acacia caesia* were collected from in and around of Rajahmundry, Andhra Pradesh, India and morphology confirmed through literature. The leaves were washed with running tap water followed by double distilled water, shade dried and made into fine powder. 1% of leaf powder was dissolved in distilled water and incubated for 20 minutes at 60°C with continuous stirring, and allowed to cool down to room temperature. The obtained solution subjected to filtration using muslin cloth followed by Whatman No 1 filter paper and ACLAE was stored at 4°C until further use [27].

2.4. Phytochemical investigation of ACLAE:

The ACLAE was subjected to Qualitative phytochemical investigation and Total polyphenol content estimation according to the [28].

2.4.1. Qualitative phytochemical investigation:

The qualitative phytochemical investigation includes identification of Flavonoids, Phenols, Tannins, Alkaloids (Mayer's and Wagner's), Terpenoids, Anthraquinones, Saponins, Quinones, Coumarins, Glycosides and Steroids.

2.4.2. Total polyphenol content (TPC) estimation:

The TPC was estimated by dissolving 10mg of dried ACLAE in 5% DMSO and filtered using Whatman No 1 filter paper. To this 10% Folin-Ciocalteu reagent and 7.5% of sodium carbonate were added. The resulting solutions were incubated for 2 hours at room temperature and absorbance was read at 765nm. Gallic acid was used as standard.

2.5. Green synthesis of ACLAE-Fe_3O_4 Nanoparticles:

The precursors $FeCl_3$ and $FeSO_4$ were dissolved in 90mL of distilled water in 1:2 ratio. 10mL of ACLAE was slowly released into the above solution under magnetic stirring at 70°C. The change in color of reaction mixture was observed from pale yellow to dark brown. Then, 10mL of 25% of ammonium hydroxide was added into the above reaction mixture for precipitation of ACLAE-Fe_3O_4 NPs. The obtained precipitate was centrifuged, pellet washed twice with distilled water followed by 70% ethyl alcohol and dried at 70°C in hot air oven [10].

2.6. Characterization of ACLAE-Fe_3O_4 NPs:

The absorbance of ACLAE and ACLAE-Fe_3O_4 NPs were analyzed using UV-Vis spectrophotometer from 200-800nm wavelength. The functional groups responsible for the reduction and capping of ACLAE and ACLAE-Fe_3O_4 NPs were analyzed using FTIR from 400-4000cm^{-1}. The average crystalline size and crystalline structure of ACLAE-Fe_3O_4 NPs were determined using powder XRD with monochromatic Cu Kα radiation (K= 1.5406 Å) operated at 30mA and 40 KV from 10 to 90° in 2θ angles. The shape and elemental compositions of ACLAE-Fe_3O_4 NPs were analyzed using FESEM coupled with EDX. The size distribution and morphology were determined using HRTEM operated at 200kV [29].

2.7. Anti-fungal activity of ACLAE-Fe_3O_4 NPs:

The antifungal activity of ACLAE-Fe_3O_4 NPs evaluated using Microdilution broth (MDB) and Disc diffusion assay. The ACLAE-Fe_3O_4 NPs were dissolved in 5% DMSO and sonicated for 60 minutes prior to experiment.

2.7.1. Micro Dilution Broth:

MDB was used to determine the Minimum Inhibitory Concentration (MIC) of ACLAE-Fe_3O_4 NPs against *Aspergillus niger* (MTCC 282) and *Candida albicans* (MTCC 183) using 96 well microtiter plate method. The concentrations of ACLAE-Fe_3O_4 NPs used were 1000-3.9 µg mL^{-1} and the fungal dilution was 10^5 CFU mL^{-1} in LB Broth. 1% TTC solution was added into all the wells. A positive and negative controls were maintained. The microtiter plates were incubated at 37°C for 24 hrs. The MIC was evaluated visually and the change in color of broth (Colorless to red) indicates the presence of bacterial growth.

2.7.2. Disc diffusion assay:

In this method 10^5 CFU mL^{-1} of each fungal culture was inoculated on MHA modified 2% glucose W/methylene blue agar. The discs were immersed in amphotericin B (Positive control-100 µg), 5% DMSO (Negative control), ACLAE (100µg) and ACLAE-Fe_3O_4 NPs (100µg) placed on MHA agar. The plates were incubated for 24 hrs at 37°C and the zone of inhibitions were measured.

2.8. *In vitro* anti-oxidant activity of ACLAE-Fe_3O_4 NPs:

The antioxidant properties of ACLAE-Fe_3O_4 NPs were evaluated using three different *in vitro* methods: DPPH free radical scavenging activity, Ferric reducing antioxidant power assay and ABTS cationic radical scavenging activity. The concentrations of ACLAE-Fe_3O_4 NPs used were 500-2000µg mL^{-1}.

In DPPH assay, various concentrations of ACLAE-Fe_3O_4 NPs in methanol were added to the 3×10^{-5}M DPPH in methanol. DPPH with methanol was used as control. In FRAP assay, various concentrations of ACLAE-Fe_3O_4 NPs in acetate buffer were added to the FRAP reagent (0.010M TPTZ in 0.040M HCl, 0.020M FeCl3 and 0.3M acetate buffer (pH 3.6) in 1:1:10 (v/v/v) proportion). FRAP with acetate buffer was used as control. In ABTS assay various concentrations of ACLAE-Fe_3O_4 NPs in distilled water were added to the ABTS reagent (7mM ABTS and 2.45mM Potassium persulphate in 1:1 ratio). The reagent was pre-incubated overnight in dark and diluted in methanol. The distilled water with ABTS reagents was used as control.

All the reaction mixtures were incubated in dark for 3 hours and centrifuged at 5000 rpm for 5 minutes at 4°C. The absorbance of supernatant was read at 517nm, 593nm and 734nm for DPPH, FRAP and ABTS assays respectively. Ascorbic acid was used as standard.

The percentage of Inhibition was calculated as follows:

$$\text{Percentage of Inhibition } (\%) = \frac{A0-A1}{A0} \times 100 \quad \textbf{(1)}$$

A0 = Absorbance of Control

A1 = Absorbance of Sample at each concentration.

The Inhibitory concentration 50 (IC_{50}) value was determined using the formula IC_{50} (0.5-b)/a **(2)**

2.9. *In vitro* anti-inflammatory activity of ACLAE-Fe_3O_4 NPs:

The anti-inflammatory activity of ACLAE-Fe_3O_4 NPs evaluated using three different *in vitro* methods i.e., Inhibition of protein denaturation, Inhibition of proteinase denaturation and RBC heat induced hemolysis assays. The concentrations of ACLAE-Fe_3O_4 NPs used were 500-2000µg mL^{-1}.

In Proteinase denaturation inhibition assay, the reaction mixtures (0.05mg trypsin, Tris HCl (pH 7.4), and various concentrations of ACLAE-Fe_3O_4 NPs) were incubated at 37°C for 5 minutes and 48 µg of casein hydrolysate was added to all reaction mixtures and incubated for further 20 minutes at 37°C. The reaction was terminated by adding 70% perchloric acid. The samples were cooled down and

centrifuged at 3000rpm for 5 mins, and the absorbance of supernatant was read at 210nm and Phosphate buffer solution was used as control.

In protein denaturation inhibition assay, the reaction mixtures (Phosphate buffer saline 6.4, 1% BSA and various concentrations of ACLAE-Fe_3O_4 NPs) were incubated at 37°C for 15 minutes and then further heated at 70°C for 5 minutes. The solutions allowed to cool down to room temperature and turbidity was measured at 660nm and Phosphate buffer solution was used as control.

In heat induced hemolysis, the heparinized chicken blood was centrifuged at 5000 rpm for 5 minutes, the supernatant was removed and washed thrice with equal volume of physiological saline (0.9% NaCl). The obtained blood volume was resuspended in 10% PBS (7.4) (v/v). Then, the reaction mixtures (Blood suspension, PBS 7.4 and various concentrations of ACLAE-Fe_3O_4 NPs) were incubated at 54°C for 20 minutes in shaking water bath and centrifuged at 2500 rpm for 5 minutes. The absorbance of supernatant was read at 540nm and Phosphate buffer solution was used as control. Diclofenac sodium was used standard for all three experiments.

The % of inhibition of proteinase denaturation was calculated according to the formula (1).

The Inhibitory concentration 50 (IC_{50}) value was determined using the formula IC_{50} (0.5-b)/a **(2).**

2.10. Cytotoxicity assay:

The cytotoxic effect of ACLAE-Fe_3O_4 NPs was evaluated on HeLa cell lines (Human cervical cancer cell lines) using MTT assay. The cultured cell lines were treated with different concentrations of ACLAE-Fe_3O_4 NPs (0 (control), 12.5, 25, 50, 100 and 200 µg mL^{-1}) in 96 well micro titre plates and incubated at 37°C in CO_2 incubator. After 48 hours of incubation the cells were treated with MTT assay and absorbance was read at 540nm using lark-LIPR 96 well micro titre ELISA reader. The cytotoxicity was calculated as follows:

Cytotoxicity $= \frac{A-B}{A} \times 100$

Where A = mean optical density of control well

B = was the optical density of treatment well.

The graph plotted with % of cell viability against concentration of ACLAE-Fe_3O_4 NPs.

The Inhibitory concentration 50 (IC_{50}) value was determined using the formula IC_{50} (0.5-b)/a.

3. RESULT AND DISCUSSION:

3.1. Phytochemical investigation:

The preliminary phytochemical investigation of ACLAE reveals the presence of alkaloids, flavonoids, tannins, phenols and estimated TPC was 120 mg/ 100 mg of gallic acid equivalent (GAE). This finding is supported by previous reports of [23] [24]. The reduction process of metal oxide nanoparticles is carried out by the phytochemicals present in the plants and can act as capping agents. The synergism of metal/metal oxides and phytochemicals increases the biological potential two fold [30].

3.2. Characterization of ACLAE-Fe_3O_4 NPs:

3.2.1. UV-Vis spectroscopy:

In the present study, the appearance of dark color after addition of ACLAE to the precursors $FeCl_3$ and $FeSO_4$ is due to surface plasmon resonance excitation and confirmed the reduction of metal oxide nanoparticles. The formation of ACLAE-Fe_3O_4 NPs was further confirmed by UV-Vis spectroscopy and prior to synthesis the absorbance of the ACLAE was also represented in fig.1. The ACLAE shown absorbance peaks between 200-300 nm wavelength range, which are characteristic peaks of phytochemical moieties. The characteristic peak for ACLAE-Fe_3O_4 NPs was found at 276 nm and no absorbance recorded after 400 nm wavelength range indicates complete reduction and

formation of IONPs. In contrast to this Fe_3O_4 NPs synthesized using *Hibiscus rosa sinensis* flowers shown absorbance peak at 229 nm [10].

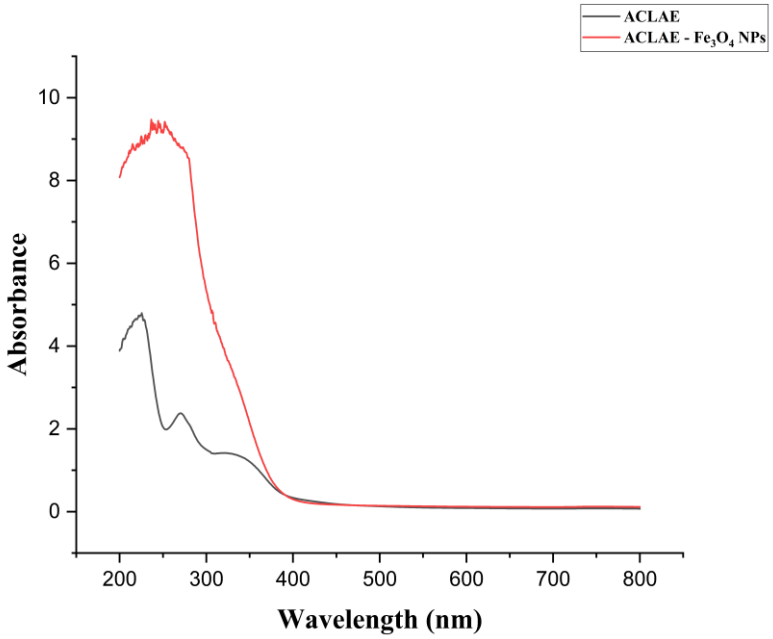

Figure 1: UV-Visible spectra of ACLAE (black) and ACLAE-Fe3O4-NPs (red).

3.2.2. FTIR: The functional groups of ACLAE and the functional groups associated with reduction and capping of ACLAE-Fe_3O_4 NPs were subjected to FTIR analysis from the range of 500-4000 cm^{-1} and the spectra (Fig.2) shows multiple vibrational signals. The ACLAE shows vibrational signals at 3250-3360 cm^{-1} corresponds to strong and broad O-H stretching, 2100 cm^{-1} corresponds to weak C≡C stretching, 1630 cm^{-1} corresponds to medium C=C stretching and 509 cm^{-1} corresponds to strong C-I stretching. The ACLAE-Fe_3O_4 NPs shows vibrational signals at 1724 cm^{-1} corresponds to strong C=O stretching, 1368 cm^{-1} corresponds to medium O-H bending, 1281 and 1118 cm^{-1} corresponds to strong C-O stretching and the weak vibrational signals at 743 and 541 cm^{-1} corresponds to metal oxide bonds in ACLAE-Fe_3O_4 NPs (1). The absence of O-H stretching in ACLAE-Fe_3O_4 NPs may be due to absence of moisture in it. The phenyl groups and polyphenols play significant reduction role in converting iron ions to IONPs [10].

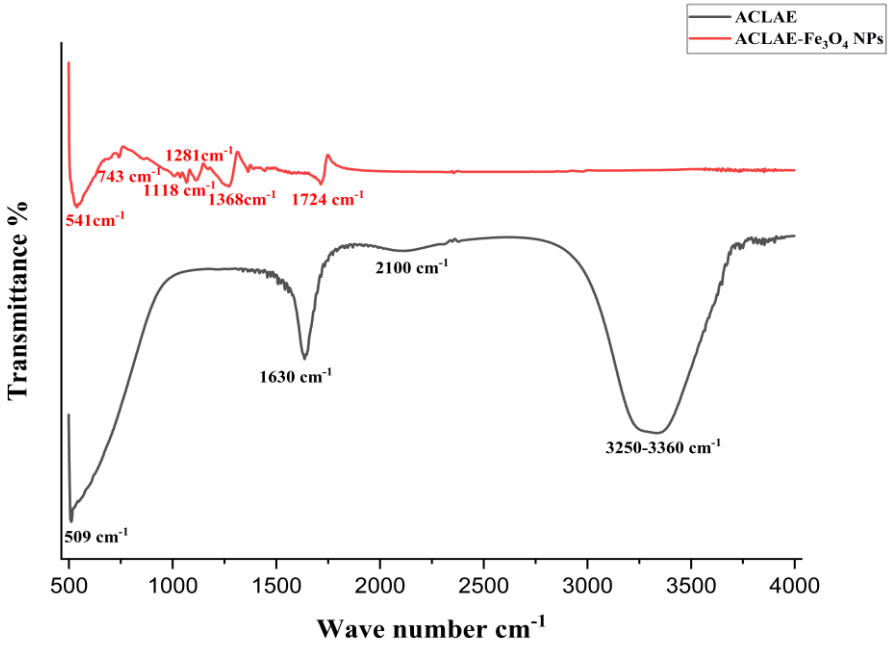

Figure 2: FTIR spectra of ACLAE (black) and ACLAE-Fe3O4 NPs (red).

3.2.3. XRD:

The crystalline nature, average crystalline size and phase identification were evaluated using XRD analysis. The long intense and broad random diffraction peaks confirmed both crystalline and amorphous nature of ACLAE-Fe_3O_4 NPs. The calculated average crystalline size was 36.24nm. The observed diffraction peaks with 2θ values of 29.84°, 35.16°, 42.73°, 56.45°, 62.07° corresponds to hkl values of 220, 311, 400, 511 and 440 respectively and revealed face cubic centered (fcc) structure represented in figure 3. The XRD data in the present study consistence with standard JCPDS magnetite structure card No. 01-089-0951 and results are correlated with previous reports [31, 32].

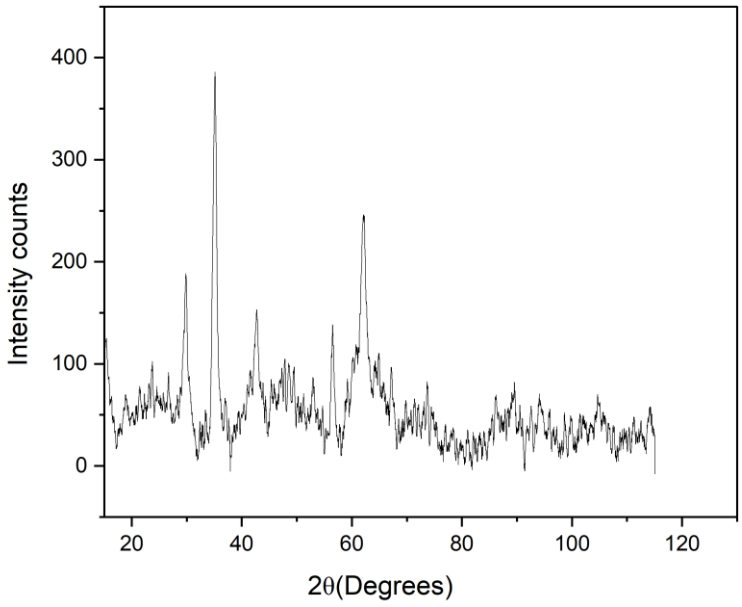

Figure 3: XRD diffraction spectrum of ACLAE-Fe_3O_4 NPs

3.2.4. FESEM and EDX:

The surface morphology, elemental composition and elemental mapping of ACLAE-Fe_3O_4 NPs established using FESEM coupled with EDX. The FESEM analysis shows that moderate agglomeration and most of them are partly spherical in shape (fig.4.(a)) of ACLAE-Fe_3O_4 NPs. The agglomeration is attributed to the magnetic properties of ACLAE-Fe_3O_4 NPs. The morphology (shape and size) of ACLAE-Fe_3O_4 NPs greatly influenced by the polyphenols in ACLAE [1].

The EDX spectrum shows characteristic peak of elements O, Fe and Mn with weight percentages 25.43%, 73.89% and 0.68% (fig.4 (b-c)) respectively and presence of Mn may be traces from ACLAE.

4(a)

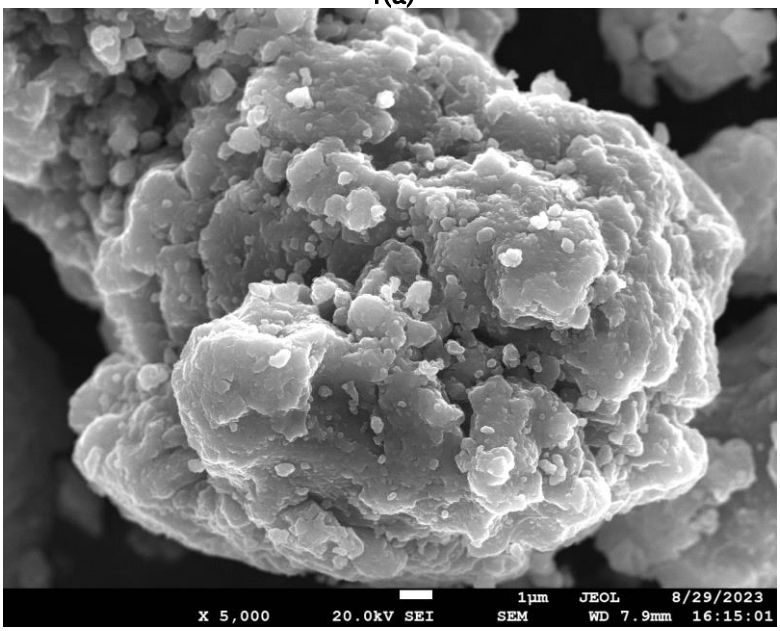

4(b)

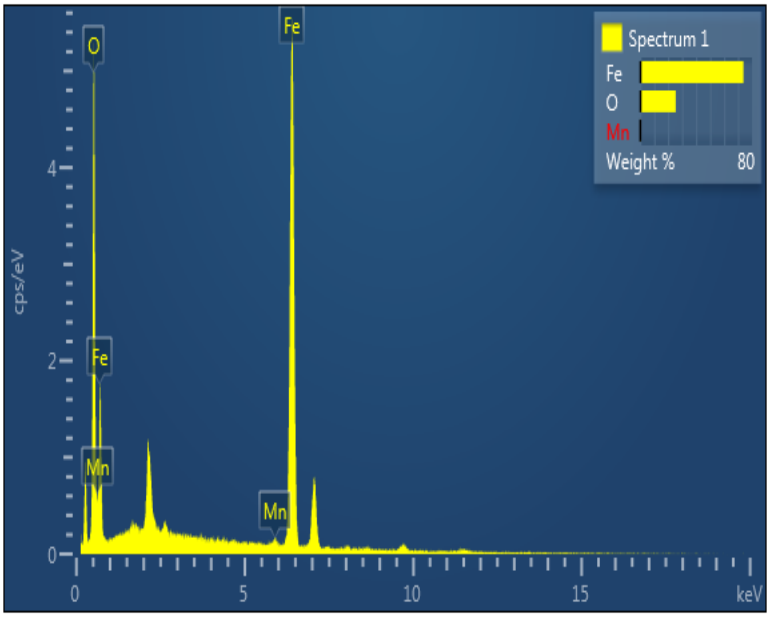

4(c)

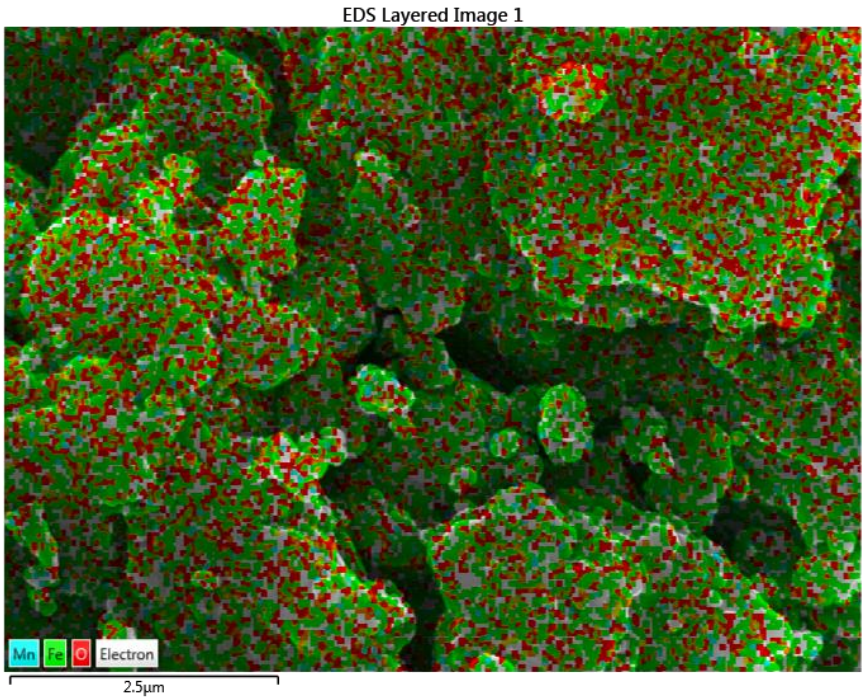

Figure 4: FESEM coupled with EDX analysis of ACLAE-Fe_3O_4 NPs, (a) FESEM surface morphology, (b) EDX spectrum (c) Elemental mapping.

3.2.5. HRTEM: The HRTEM analysis was employed to adjudge the particle size distribution and Selected Area Diffraction (SAED) pattern of ACLAE-Fe_3O_4 NPs. The morphology, particle size distribution and SAED pattern are represented in Fig.5 a-c. The particles are partly spherical in shape and calculated average particle size is 69nm, the particles with >100nm are resulted due to more accumulation of phytochemicals on precursor ions. The diffraction rings of SAED pattern corresponds to monocrystalline nature of NPs and are correlated with XRD diffraction peaks.

5(a)

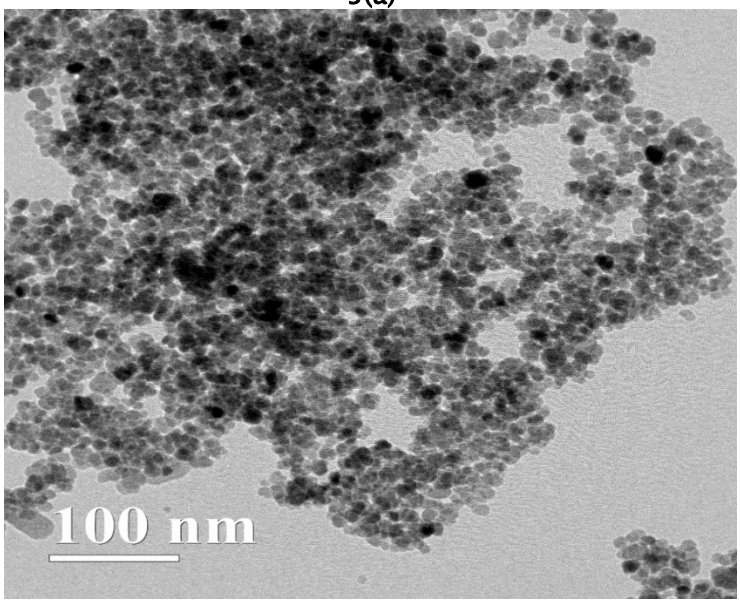

5(b)

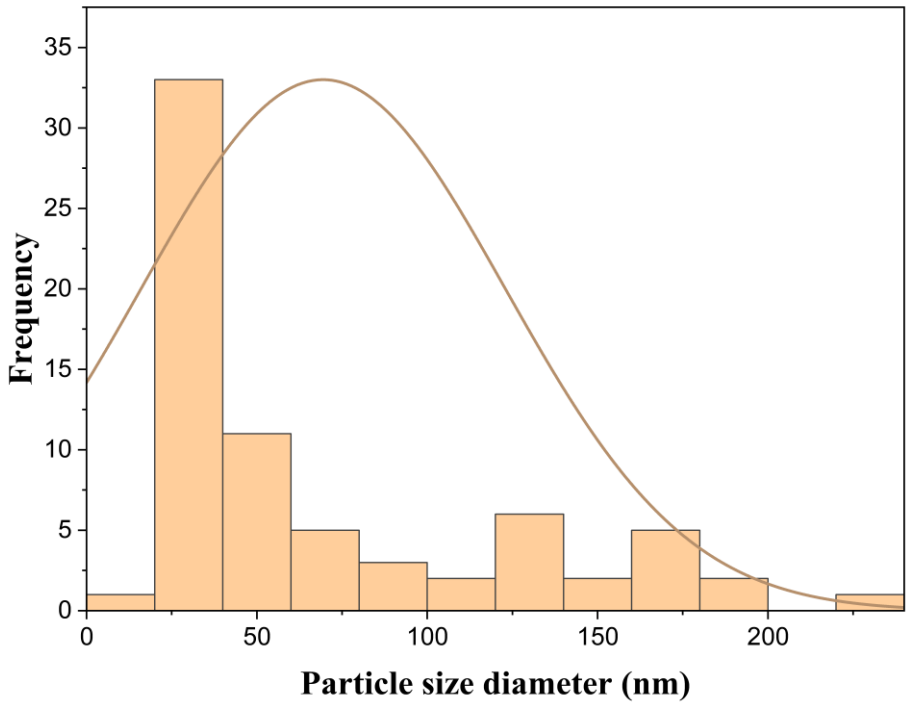

5(c)

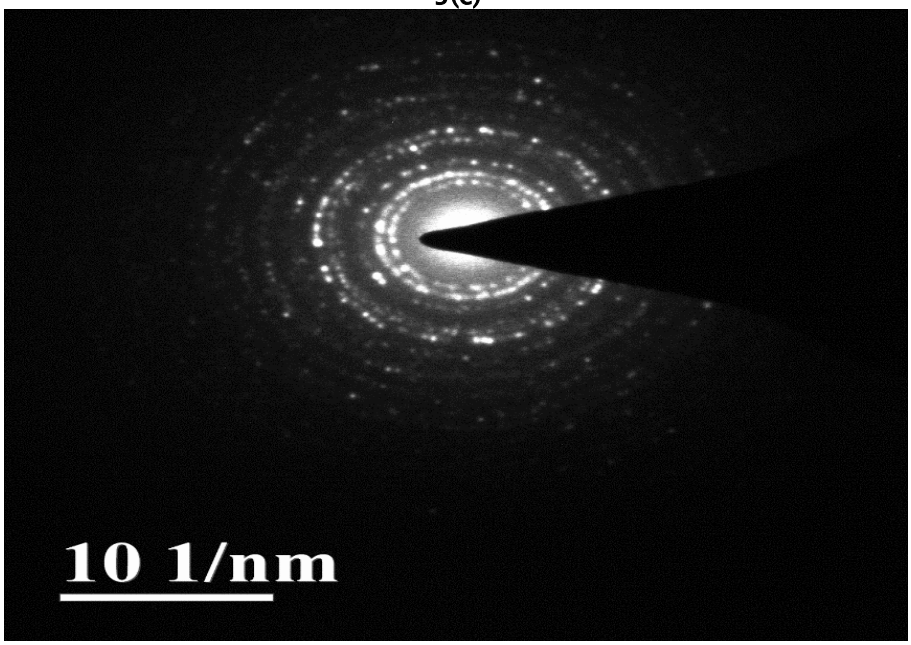

Figure 5: HRTEM Micrograph analysis of Fe_3O_4 NPs (a) TEM micrograph (b) Particle size distribution (c) SAED pattern.

3.3. Anti-fungal activity:

The development of antifungal resistance has been called "Unprecedented" and one of the causes for worldwide mortality [33]. The antifungal resistance arises due to biofilm formation [34], efflux pump synthesis [35], alteration in gene expression [36], target site modification [37] etc., The immunocompromised patients are prone to fungal infections than healthy individuals. In this bizarre,

there is a need for development of novel antifungal to combat the increasing resistance towards the conventional antifungals. Metal NPs/Metal oxide NPs may become repurposing antifungals because they exhibit numerous mechanisms of action and fungi would have to develop resistance in multiple ways [33].

In the present study, the anti-fungal activity revealed that, the ACLAE does not shown any activity at 100 µg concentration whereas ACLAE-Fe_3O_4 NPs shown moderate zone of inhibition against *Candida* (10mm) and *Aspergillus* (12mm) which are lower than the standard antifungal agent Amphotericin B. The microdilution broth assay revealed similar MIC of ACLAE-$Fe3O_4$ NPs against both *Candida* and *Aspergillus* which is 125 µg mL^{-1}. The results of the present study are represented in table 2. Similar study reported antifungal properties of IONPs [18].

Table 2: Antifungal activity of Amphotericin B/ACLAE/ /ACLAE-$Fe3O_4$ NPs

Zone of Inhibition (mm)		
Amphotericin B/ACLAE/ /ACLAE-$Fe3O_4$ NPs (100 µg)	***Candida albicans*** **Mean ± SD**	***Aspergillus niger*** **Mean ± SD**
Amphotericin B	18 ± 0	20 ± 0
ACLAE	0	0
ACLAE- $Fe3O_4$ NPs	10 ± 0	12 ± 0
Minimum Inhibitory Concentration (MIC) µg mL^{-1}		
ACLAE- $Fe3O_4$ NPs	125 ± 0	125 ± 0

3.4. *In vitro* antioxidant activity: The DPPH free radical scavenging, ferric reducing and ABTS cationic scavenging activity assays were used to evaluate the antioxidant properties of ACLAE-Fe_3O_4 NPs. The concentration dependent activities and IC_{50} values were given in table 3.

The imbalanced reactive oxygen/nitrogen species (ROS/RNS) and antioxidant activity result in oxidative stress which is one of the key causes for several diseases. The IONPs are excellent scavengers of ROS/RNS, however the activity is depends on the precursor and fabrication molecule [38].

The three *in vitro* activities revealed effective antioxidant properties with maximum percentage of inhibitions of 88.58%, 71.83% and 82.50% for DPPH, FRAP and ABTS assays at 2000 µg mL^{-1} concentration respectively. The IC_{50} values of three assays are quite vary and ABTS showed highest IC_{50} value of 3546 µg mL^{-1}, indicates requirement of higher ACLAE-Fe_3O_4 NPs concentration for cationic radical scavenging activity. Fabrication of IONPs with natural antioxidants shown excellent antioxidant properties [39].

Table 3: *invitro* anti-oxidant activity of ACLAE-Fe_3O_4 NPs.

Concentration dependent % of activity			
Concentration of ACLAE-$Fe3O_4$ NPs (µg mL^{-1})	DPPH free radical scavenging activity (%) Mean ± SD	Ferric reducing antioxidant activity (%) Mean ± SD	ABTS cationic radical scavenging activity (%) Mean ± SD
500	63.27 ± 0.018	37.64 ± 0.075	32.21 ± 0.047
1000	74.38 ± 0.012	60.44 ± 0.014	57.14 ± 1.12
1500	83.33 ± 0.05	65.26 ± 0.075	64.72 ± 0
2000	88.58 ± 0.012	71.83 ± 0	82.50 ± 0.047
IC_{50} ranges (µg mL^{-1})			
IC_{50} ranges	845	673	3546

3.5. *In vitro* anti-inflammatory activity:

The *in vitro* anti-inflammatory activities of ACLAE-Fe_3O_4 NPs were evaluated using three different assays: Inhibition of albumin denaturation, Inhibition of Head induced RBC hemolysis and Inhibition of proteinase denaturation. The concentration dependent % of inhibition and the IC_{50} values were given in table 4.

Conventional non-steroidal anti-inflammatory drugs (NSAIDs) are involved in blocking the inflammatory enzymes produced during various physiological and pathological processes, but associated with adverse side effects. During the inflammation, there is an increase of protein denaturation, vascular permeability and cell membrane alteration [40]. The ACLAE-Fe_3O_4 NPs in the present study shown effective inhibition of albumin denaturation with maximum percentage of inhibition of 84.08% at 2000 µg mL^{-1}. Surprisingly the similar percentage for inhibition of albumin denaturation found at both 1500 and 2000µg mL^{-1} concentration anti-inflammatory activity which indicates the saturation level of ACLAE-Fe_3O_4 NPs for inhibition of albumin denaturation activity.

As a part of their defensive role, WBC cells release lysosomal proteases which cause tissue damage and eventually the cells become susceptible to the secondary damage (eg., lipid peroxidation). The heat induced RBC membrane hemolysis inhibition assay is used to evaluate inhibitory properties of synthetic drugs/natural products and the RBC membrane composition is similar to the lysosomes of WBC[41, 42]. In this study, the inhibition of heat induced RBC membrane hemolysis and inhibition of proteinase denaturation by ACLAE-Fe_3O_4 NPs shown maximum percentage of inhibition of 22.45% and 38.98% respectively at 2000 µg mL^{-1}. This indicates the requirement of higher concentrations of ACLAE-Fe_3O_4 NPs to achieve the maximum % of inhibition and may correlate with more cytotoxicity. Inhibition of lysis can minimize the tissue damage and inhibition of inflammatory progression in various pathological process [43].

The IC_{50} value indicates that, the specific concentration of ACLAE-Fe_3O_4 NPs is required to inhibit the 50% of activity. Among three assays Inhibition of protein denaturation showed lowest IC_{50} value (996 µg mL^{-1}) whereas Inhibition of proteinase denaturation showed highest IC_{50} value (1531 µg mL^{-1}).

Table 4: *invitro* anti-inflammatory activity of ACLAE-Fe_3O_4 NPs

Concentration dependent % of Inhibitory activity			
Concentration of ACLAE-Fe_3O_4 NPs (µg mL^{-1})	Inhibition of Protein denaturation (%) Mean ± SD	Inhibition of heat induced RBC hemolysis (%) Mean ± SD	Inhibition of Proteinase denaturation (%) Mean ± SD
500	70.78 ± 0	2.22 ± 0.070	23.41 ± 0.063
1000	77.67 ± 0.056	10.76 ± 0.267	25.19 ± 0.028
1500	84.08 ± 0.075	19.76 ± 0.075	32.53 ± 0
2000	84.08 ± 0.028	22.45 ± 0	38.98 ± 0.195
IC_{50} ranges (µg mL^{-1})			
IC_{50} ranges	996	1075	1531

3.6. Cytotoxicity:

In the present study, the cytotoxicity of ACLAE-Fe_3O_4 NPs was evaluated against HeLa cell lines (Human cervical cancer cell lines). The depicted Fig.6&7 represents the concentration dependent cell cytotoxicity and the maximum cell death (48.86%) was observed at 200 µg mL^{-1} after 48 hours of incubation and calculated IC_{50} value was 65.30 µg mL^{-1} which indicates that the cytotoxicity can be

achieved using lower concentrations of ACLAE-Fe_3O_4 NPs. The increased cytotoxicity of HeLa cell lines due to generation of oxidative damage (Protein and DNA damage) eventually leads to apoptosis. Therefore, the IONPs are strong inducers of oxidative damage in cancer cell lines [12]. The further studies required to understand the IONPs mechanism of toxicity and toxicity towards healthy cell lines.

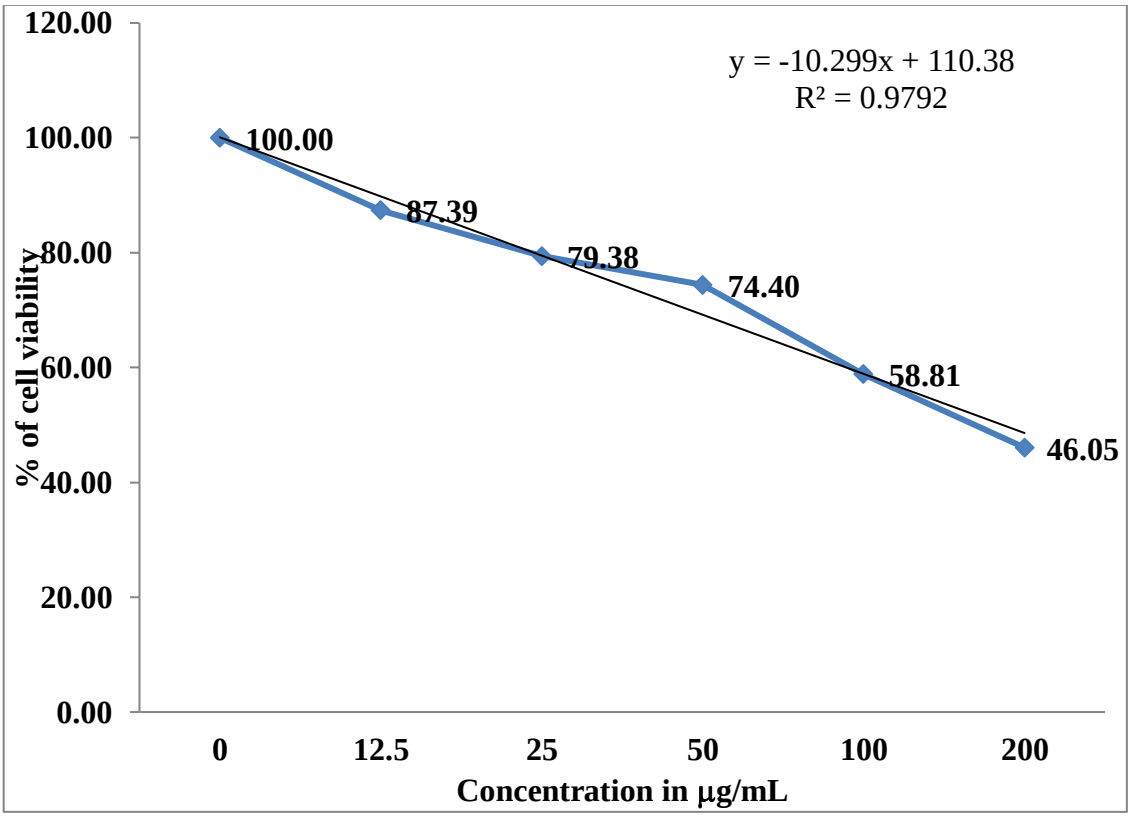

Figure 6: Concentration dependent cytotoxicity of ACLAE-Fe_3O_4 NPs on HeLa cell lines.

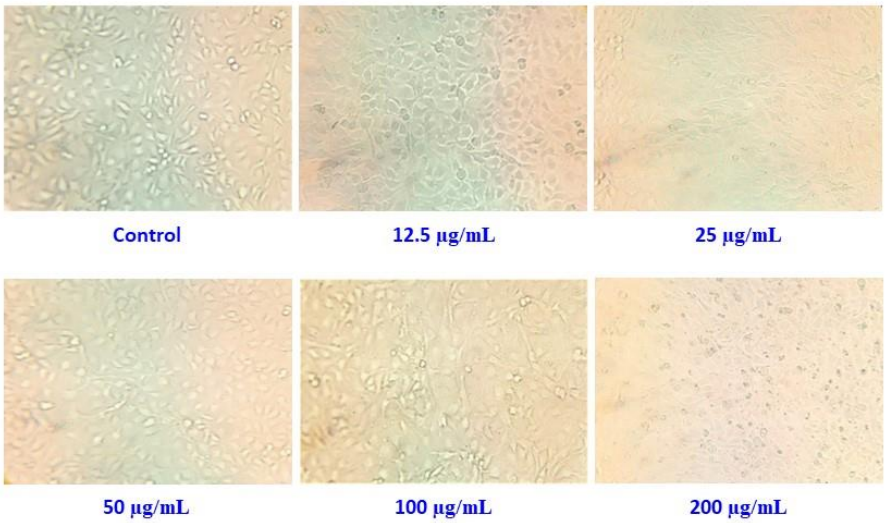

Figure 7: Morphology of HeLa cells treated with different concentrations of ACLAE-Fe_3O_4 NPs.

Conclusion:

The sustainable synthesis of magnetite nanoparticles using green resources is simple, ecofriendly, cost effective and does not involve use of any harmful chemicals. In the present study, the green synthesis of Fe_3O_4 NPs using *Acacia caesia* leaf aqueous extract (ACLAE) as reducing and capping agent and its biological activities such as anti-fungal, *in vitro* antioxidant and anti-inflammatory properties has been successfully demonstrated. A comparative antifungal activity between ACLAE and ACLAE- Fe_3O_4 NPs has been determined, in which ACLAE- Fe_3O_4 NPs shown effective antifungal property. The ACLAE- Fe_3O_4 NPs are effective in neutralizing the free radicals which are evaluated using *invitro* DPPH, FRAP and ABTS antioxidant assays and also shows effective *in vitro* anti-inflammatory activity, inhibitory property against albumin denaturation, RBC hemolysis and Proteinase denaturation. The cytotoxicity assay revealed highest % of cell death with lower IC_{50} value on HeLa cell lines. The striking feature of the current study is to develop environmentally benign nanomaterials for various biomedical applications. The current study is only limited to *in vitro* evaluation of biological activities and future studies required to understand the correlation between antioxidant activity and generation of oxidative stress in healthy cells. The environmental safety evaluation in terms of toxicity towards the beneficial organisms of soil and aquatic environments is required.

Abbreviations:

Fe_3O_4 – Magnetite Nanoparticles
ACLAE – *Acacia caesia* leaf aqueous extract
IONPs – Iron oxide Nanoparticles
RBC – Red blood cells
WBC – White blood cells

Acknowledgements:

The authors are thankful to DST-FIST coordinator, Central Instrumentation Laboratory (CIL), Government college (A), Rajahmundry for providing research space for smooth conduction of experimental work.

Author Contribution:

Shyamala Pulipaka: Supervision, conceptualization, editing and reviewing of manuscript
Machiraju Padmaja: Methodology, resources, investigation and manuscript writing.

Data Availability:

Addressed to Shyamala Pulipaka

Declarations

Competing and Conflict of interest: The authors declare no competing and conflict of interest.

Ethics Approval and Consent to Participate: Not applicable.

Consent for Publication: Not applicable.

Research Involving Humans and Animals Statement: The article does not contain any studies involving human participants and animals performed by any of the authors.

Informed Consent: Not Applicable.

References:

1. Jain, R., Mendiratta, S., Kumar, L., & Srivastava, A. (2021). Green synthesis of iron nanoparticles using Artocarpus heterophyllus peel extract and their application as a heterogeneous Fenton-like catalyst for the degradation of Fuchsin Basic dye. *Current Research in Green and Sustainable Chemistry*, *4*(March), 100086. https://doi.org/10.1016/j.crgsc.2021.100086
2. Demirezen, D. A., Yılmaz, Ş., Yılmaz, D. D., & Yıldız, Y. Ş. (2022). Green synthesis of iron oxide nanoparticles using Ceratonia siliqua L. aqueous extract: improvement of colloidal stability by optimizing synthesis parameters, and evaluation of antibacterial activity against Gram-positive and Gram-negative bacteria. *International Journal of Materials Research*, *113*(10), 849–861. https://doi.org/10.1515/ijmr-2022-0037
3. Üstün, E., Önbaş, S. C., Çelik, S. K., Ayvaz, M. Ç., & Şahin, N. (2022). Green synthesis of iron oxide nanoparticles by using ficus carica leaf extract and its antioxidant activity. *Biointerface Research in Applied Chemistry*, *12*(2), 2108–2116. https://doi.org/10.33263/BRIAC122.21082116
4. AL-Husseini, A. H., Sih, B. T., & Al-Araji, A. M. (2021). Green synthesis of iron oxide nanoparticles (Fe2O3) using saffron extract. *Journal of Physics: Conference Series*, *2114*(1). https://doi.org/10.1088/1742-6596/2114/1/012082
5. Leaves, L., & Dyes, O. (2022). Green Synthesis of Iron Oxide Nanoparticles Using Psidium.
6. Priya, Naveen, Kaur, K., & Sidhu, A. K. (2021). Green Synthesis: An Eco-friendly Route for the Synthesis of Iron Oxide Nanoparticles. *Frontiers in Nanotechnology*, *3*(June). https://doi.org/10.3389/fnano.2021.655062
7. Buarki, F., AbuHassan, H., Al Hannan, F., & Henari, F. Z. (2022). Green Synthesis of Iron Oxide Nanoparticles Using Hibiscus rosa sinensis Flowers and Their Antibacterial Activity. *Journal of Nanotechnology*, *2022*, 1–6. https://doi.org/10.1155/2022/5474645
8. Saif, S., Tahir, A., & Chen, Y. (2016). Green synthesis of iron nanoparticles and their environmental applications and implications. *Nanomaterials*, *6*(11), 1–26. https://doi.org/10.3390/nano6110209
9. Arias, L. S., Pessan, J. P., Vieira, A. P. M., De Lima, T. M. T., Delbem, A. C. B., & Monteiro, D. R. (2018). Iron oxide nanoparticles for biomedical applications: A perspective on synthesis, drugs, antimicrobial activity, and toxicity. *Antibiotics*, *7*(2). https://doi.org/10.3390/antibiotics7020046
10. Razack, S. A., Suresh, A., Sriram, S., Ramakrishnan, G., Sadanandham, S., Veerasamy, M., … Sahadevan, R. (2020). Green synthesis of iron oxide nanoparticles using Hibiscus rosa-sinensis for fortifying wheat biscuits. *SN Applied Sciences*, *2*(5), 1–9. https://doi.org/10.1007/s42452-020-2477-x
11. Singh, K., Chopra, D. S., Singh, D., & Singh, N. (2022). Green synthesis and characterization of iron oxide nanoparticles using Coriandrum sativum L. leaf extract. *Indian Journal of Biochemistry and Biophysics*, *59*(4), 450–454. https://doi.org/10.56042/ijbb.v59i4.61913
12. Bhuiyan, M. S. H., Miah, M. Y., Paul, S. C., Aka, T. Das, Saha, O., Rahaman, M. M., … Ashaduzzaman, M. (2020). Green synthesis of iron oxide nanoparticle using Carica papaya leaf extract: application for photocatalytic degradation of remazol yellow RR dye and antibacterial activity. *Heliyon*, *6*(8), e04603. https://doi.org/10.1016/j.heliyon.2020.e04603

13. Kiwumulo, H. F., Muwonge, H., Ibingira, C., Lubwama, M., Kirabira, J. B., & Ssekitoleko, R. T. (2022). Green synthesis and characterization of iron-oxide nanoparticles using Moringa oleifera: a potential protocol for use in low and middle income countries. *BMC Research Notes*, *15*(1), 1-8. https://doi.org/10.1186/s13104-022-06039-7
14. Lakshmnarayanan, S., Shereen, M. F., Niraimathi, K. L., Brindha, P., & Arumugam, A. (2021). One-pot green synthesis of iron oxide nanoparticles from Bauhinia tomentosa: Characterization and application towards synthesis of 1, 3 diolein. *Scientific Reports*, *11*(1), 1-13. https://doi.org/10.1038/s41598-021-87960-y
15. Azizi, A. (2020). Green Synthesis of Fe3O4 Nanoparticles and Its Application in Preparation of Fe3O4/Cellulose Magnetic Nanocomposite: A Suitable Proposal for Drug Delivery Systems. *Journal of Inorganic and Organometallic Polymers and Materials*, *30*(9), 3552-3561. https://doi.org/10.1007/s10904-020-01500-1
16. Arsalani, S., Guidelli, E. J., Araujo, J. F. D. F., Bruno, A. C., & Baffa, O. (2018). Green Synthesis and Surface Modification of Iron Oxide Nanoparticles with Enhanced Magnetization Using Natural Rubber Latex. *ACS Sustainable Chemistry and Engineering*, *6*(11), 13756-13765. https://doi.org/10.1021/acssuschemeng.8b01689
17. Yusefi, M., Shameli, K., Yee, O. S., Teow, S. Y., Hedayatnasab, Z., Jahangirian, H., … Kuča, K. (2021). Green synthesis of fe3o4 nanoparticles stabilized by a garcinia mangostana fruit peel extract for hyperthermia and anticancer activities. *International Journal of Nanomedicine*, *16*, 2515-2532. https://doi.org/10.2147/IJN.S284134
18. Patra, J. K., & Baek, K. H. (2017). Green biosynthesis of magnetic iron oxide (Fe3O4) nanoparticles using the aqueous extracts of food processing wastes under photo-catalyzed condition and investigation of their antimicrobial and antioxidant activity. *Journal of Photochemistry and Photobiology B: Biology*, *173*, 291-300. https://doi.org/10.1016/j.jphotobiol.2017.05.045
19. Sandhya, J., & Kalaiselvam, S. (2020). Biogenic synthesis of magnetic iron oxide nanoparticles using inedible borassus flabellifer seed coat: Characterization, antimicrobial, antioxidant activity and in vitro cytotoxicity analysis. *Materials Research Express*, *7*(1). https://doi.org/10.1088/2053-1591/ab6642
20. Shi, H., Tan, L., Du, Q., Chen, X., Li, L., Liu, T., … Meng, X. (2014). Green synthesis of Fe3O4 nanoparticles with controlled morphologies using urease and their application in dye adsorption. *Dalton Transactions*, *43*(33), 12474-12479. https://doi.org/10.1039/c4dt01161a
21. Zakariya, N. A., Majeed, S., & Jusof, W. H. W. (2022). Investigation of antioxidant and antibacterial activity of iron oxide nanoparticles (IONPS) synthesized from the aqueous extract of Penicillium spp. *Sensors International*, *3*(January), 1-9. https://doi.org/10.1016/j.sintl.2022.100164
22. Win, T. T., Khan, S., Bo, B., Zada, S., & Fu, P. C. (2021). Green synthesis and characterization of Fe3O4 nanoparticles using Chlorella-K01 extract for potential enhancement of plant growth stimulating and antifungal activity. *Scientific Reports*, *11*(1), 1-11. https://doi.org/10.1038/s41598-021-01538-2
23. Babu, R. A., M, T. G., TR, A., S, I., & Nair, A. S. (2020). Pharmacognostic and antibacterial activity evaluation of Acacia caesia (L.) Willd. *Journal of Pharmacognosy and Phytochemistry*, *9*(3), 48-54. Retrieved from https://www.phytojournal.com/archives/2020.v9.i3.11479/pharmacognostic-and-antibacterial-activity-evaluation-of-acacia-caesia-l-willd
24. Venkata Smitha, P., Prameela, K., Sravani, R., & Raju Akondi, B. (2012). Screening of antimicrobial and antioxidant potentials of Acacia caesia, Dillenia pentagyna and Buchanania lanzan from Maredumilli Forest of India. *J Pharm Res*, *5*(3), 1734-38. Retrieved from

https://www.researchgate.net/profile/Akondi_Butchi_Raju/publication/253816169_Screening_of_Antimicrobial_and_Antioxidant_Potentials_of_Acacia_caesia_Dillenia_pentagyna_and_Buchania_lanzan_from_Maredumilli_Forest_of_India/links/0046352bbed6024a5a000000.p

25. Benelli, G., Kadaikunnan, S., Alharbi, N. S., & Govindarajan, M. (2018). Biophysical characterization of Acacia caesia-fabricated silver nanoparticles: effectiveness on mosquito vectors of public health relevance and impact on non-target aquatic biocontrol agents. *Environmental Science and Pollution Research*, *25*(11), 10228–10242. https://doi.org/10.1007/s11356-017-8482-y
26. Ashwini, J., Aswathy, T. R., Rahul, A. B., Thara, G. M., & Nair, A. S. (2021). Synthesis and characterization of zinc oxide nanoparticles using acacia caesia bark extract and its photocatalytic and antimicrobial activities. *Catalysts*, *11*(12). https://doi.org/10.3390/catal11121507
27. Al-Manhel, A. J., & Kareem Niamah, A. (2012). Effect of Aqueous and Alcoholic Plant Extracts on Inhibition of Some Types of Microbes and Causing Spoilage of Food. *Journal of Nutrition & Food Sciences*, *s5*, 5–7. https://doi.org/10.4172/2155-9600.s5-006
28. Mishra, P., Yadav, K. S., & Gautam, G. (2018). COMPARATIVE QUALITATIVE AND QUANTITATIVE PHYTOCHEMICAL ANALYSIS OF CALOTROPIS GIGANTEA AND CALOTROPIS PROCERA ROOTS, *8*(4), 179–184.
29. Pangi, V. N., Marukurti, A., Reddy, A. M., & Medapalli, S. R. (2023). Synthesis of Biogenic Silver Nanoparticles (bAgNPs) Using Leaf Extract of Mirabilis jalapa and Evaluation of Anti-vibriocidal, Anti-oxidant properties and Cytotoxicity. *BioNanoScience*, (0123456789). https://doi.org/10.1007/s12668-023-01060-x
30. Adeyemi, J. O., Oriola, A. O., Onwudiwe, D. C., & Oyedeji, A. O. (2022). Plant Extracts Mediated Metal-Based Nanoparticles: Synthesis and Biological Applications. *Biomolecules*, *12*(5). https://doi.org/10.3390/biom12050627
31. Fahlepy, M. R., Tiwow, V. A., & Subaer. (2018). Characterization of magnetite (Fe3O4) minerals from natural iron sand of Bonto Kanang Village Takalar for ink powder (toner) application. *Journal of Physics: Conference Series*, *997*(1). https://doi.org/10.1088/1742-6596/997/1/012036
32. Makarov, V. V., Makarova, S. S., Love, A. J., Sinitsyna, O. V., Dudnik, A. O., Yaminsky, I. V., … Kalinina, N. O. (2014). Biosynthesis of stable iron oxide nanoparticles in aqueous extracts of hordeum vulgare and rumex acetosa plants. *Langmuir*, *30*(20), 5982–5988. https://doi.org/10.1021/la5011924
33. Slavin, Y. N., & Bach, H. (2022). Mechanisms of Antifungal Properties of Metal Nanoparticles. *Nanomaterials*, *12*(24). https://doi.org/10.3390/nano12244470
34. Chandra, J., Kuhn, D. M., Mukherjee, P. K., Hoyer, L. L., Cormick, T. M. C., & Ghannoum, M. A. (2001). Biofilm formation by the fungal pathogen Candida albicans. *Journal of Bacteriology*, *183*(18), 5385–5394. https://doi.org/10.1128/JB.183.18.5385
35. Morschhäuser, J., Barker, K. S., Liu, T. T., Blaß-Warmuth, J., Homayouni, R., & Rogers, P. D. (2007). The transcription factor Mrr1p controls expression of the MDR1 efflux pump and mediates multidrug resistance in Candida albicans. *PLoS Pathogens*, *3*(11), 1603–1616. https://doi.org/10.1371/journal.ppat.0030164
36. Vermitsky, J. P., Earhart, K. D., Smith, W. L., Homayouni, R., Edlind, T. D., & Rogers, P. D. (2006). Pdr1 regulates multidrug resistance in Candida glabrata: Gene disruption and genome-wide expression studies. *Molecular Microbiology*, *61*(3), 704–722. https://doi.org/10.1111/j.1365-2958.2006.05235.x
37. Sagatova, A. A., Keniya, M. V., Wilson, R. K., Monk, B. C., & Tyndall, J. D. A. (2015). Structural

insights into binding of the antifungal drug fluconazole to Saccharomyces cerevisiae lanosterol 14α-demethylase. *Antimicrobial Agents and Chemotherapy*, *59*(8), 4982-4989. https://doi.org/10.1128/AAC.00925-15

38. Ge, X., Cao, Z., & Chu, L. (2022). The Antioxidant Effect of the Metal and Metal-Oxide Nanoparticles. *Antioxidants (Basel, Switzerland)*, *11*(4). https://doi.org/10.3390/antiox11040791
39. Kumar, B., Smita, K., Galeas, S., Sharma, V., Guerrero, V. H., Debut, A., & Cumbal, L. (2020). Characterization and application of biosynthesized iron oxide nanoparticles using Citrus paradisi peel: A sustainable approach. *Inorganic Chemistry Communications*, *119*, 108116. https://doi.org/10.1016/j.inoche.2020.108116
40. Gunathilake, K. D. P. P., Ranaweera, K. K. D. S., & Rupasinghe, H. P. V. (2018). In vitro anti-inflammatory properties of selected green leafy vegetables. *Biomedicines*, *6*(4), 1-10. https://doi.org/10.3390/biomedicines6040107
41. Okoli, C. O., Akah, P. A., Onuoha, N. J., Okoye, T. C., Nwoye, A. C., & Nworu, C. S. (2008). Acanthus montanus: An experimental evaluation of the antimicrobial, anti-inflammatory and immunological properties of a traditional remedy for furuncles. *BMC Complementary and Alternative Medicine*, *8*(June 2014). https://doi.org/10.1186/1472-6882-8-27
42. Umapathy, E., Ndebia, E. J., Meeme, A., Adam, B., Menziwa, P., Nkeh-Chungag, B. N., & Iputo, J. E. (2010). An experimental evaluation of Albuca setosa aqueous extract on membrane stabilization, protein denaturation and white blood cell migration during acute inflammation. *Journal of Medicinal Plants Research*, *4*(9), 789-795. https://doi.org/10.5897/JMPR10.056
43. Govindappa, M., Naga Sravya, S., Poojashri, M. N., Sadananda, T. S., Chandrappa, C. P., Santoyo, G., … Anil Kumar, N. V. (2011). Antimicrobial, antioxidant and in vitro anti-inflammatory activity and phytochemical screening of water extract of wedelia trilobata (L.) hitchc. *Journal of Medicinal Plant Research*, *5*(24), 5718-5729.